Gastonguay Siu
BCHEM 4995 - Honors thesis (Sept 2019-April 2020)
Supervisor: Dr. Athanasios Zovoilis, Dept. of Chemistry and Biochemistry, University of Lethbridge
External Examiner: Dr. Trushar Patel, Dept. of Chemistry and Biochemistry, University of Lethbridge

Title:

Increased SINE B2 RNA processing correlates with increased nicotine intake in neural cells

Introduction
1.1 Background

Non-coding RNA (ncRNA) and genes play crucial roles in synaptic signalling, energy production, and protein homeostasis changes in the human brain, which are associated with aging [1]. Neurodegenerative diseases like Alzheimer's Disease (AD) and Parkinson's Disease (PD) impact ncRNA and gene expression differently than normal aging.

Alzheimer's is a complex neurodegenerative disorder characterized by a gradual decline in memory and other cognitive functions, such as communication, movement, higher visual processing, and language ability [2]. AD initially damages neurons and their connections in memory-associated brain regions, like the entorhinal cortex and hippocampus, before progressing to the cerebral cortex and other areas [3]. The primary causes of AD are extracellular beta-amyloid (Aβ42/40) aggregates that accumulate between neurons and intracellular hyperphosphorylated Tau protein, forming twisted fibres known as tangles. These factors lead to neuroinflammation and brain cell death.

Parkinson's disease, on the other hand, is a neurological disorder marked by progressive loss of dopaminergic neurons in the substantia nigra pars compacta, resulting in tremors, rigidity, and bradykinesia [4]. The principal cause of PD is the aggregation of α-synuclein protein [2]. While nigrostriatal dopaminergic deficits are the most severe, PD also involves declines in numerous other central nervous system (CNS) neurotransmitter systems, likely contributing to non-motor problems associated with the disease.

Despite differences in brain location and clinical manifestations, AD and PD share some common pathological features [5]. Both diseases exhibit similarities in neuronal nicotinic acetylcholine receptor (nAChR) involvement, prompting research into the protective effects of smoking against the development of AD and PD. Chronic nicotine intake has been proposed to slow disease progression or improve function in patients with AD or PD and serve as a neuroprotectant against certain forms of dementia [6]. This is supported by the theory that nAChR activation is related to maintaining cognitive function during aging and dementia [7]. Loss of cholinergic markers, including nicotine binding sites and nAChR subunit expression, has been observed in patients with various types of dementia, suggesting that decreased cholinergic function could contribute to cognitive deficits associated with dementia.

Glutamate toxicity may also contribute to AD, with L-glutamate (L-Glu) dysregulation causing excitotoxicity, which can kill nerve cells [8]. Excitotoxicity results from excessive activation of ionotropic glutamate receptors (iGluRs), leading to the loss of postsynaptic structures like dendrites. Altered calcium homeostasis and increased sensitivity of NMDA receptors in AD may make neurons more susceptible to excitotoxicity. The relationship between AD and PD in genomics and transcriptomics has only recently begun to be investigated.

The non-coding portion of the genome plays a significant role in cellular regulatory processes, including neural development, neural plasticity, brain aging, and central nervous system diseases [9, 10]. Epigenetic factors, such as stress and toxins, influence ncRNA expression and processing. ncRNAs are typically classified into short ncRNAs (~20–30 nt), including microRNAs (miRs); small ncRNAs (up to 200 nt); and long ncRNAs (> 200 nt) [11].

Research has increasingly implicated ncRNA, particularly miRNAs, in AD [11]. Profiling studies in human and mouse models suggest that miRNAs are differentially expressed in AD, with several miRNAs regulating key AD-related genes, including APP and BACE1. In the human brain, miR-125b and miR-128 have increased in AD patients [12], while miR-106b and miR-107 expression decreases [13]. One study identified 21 highly expressed miRNAs in the hippocampus, with miR-34c significantly upregulated in APPPS1-21 (APP) mice models associated with AD. This suggests that miR-34c upregulation in AD brains may contribute to memory deficits [11].

Long ncRNAs (lncRNAs) have also been found to play a role in AD and are differentially expressed in patients with the disease [11]. AD is caused by amyloid protein deposition of beta-amyloid Aß-42 due to abnormal APP processing. APP is processed by a group of secretases, including BACE1, which cleaves APP [13]. The lncRNA BACE1-AS (antisense transcript BACE1) regulates BACE1 mRNA and protein expression. BACE1-AS rapidly and reversibly upregulates BACE1 levels in response to stressors, including Aβ 1-42 exposure. This upregulation increases BACE1 mRNA stability and generates additional Aβ 1–42 through a post-transcriptional feed-forward mechanism. BACE1-AS levels and activity are elevated in both AD patients and APP transgenic mice, directly implicating this lncRNA in the increased accumulation of APP in AD brains. Additionally, lncRNA BC200 is deregulated in AD brains [14]. BC200 RNA is significantly upregulated in specific brain areas involved in AD, with increased expression paralleling the disease's progression. The overexpression of BC200 RNA may be a reactive or causative response to synaptodendritic deterioration in AD neurons.

Rana et al. [2] investigated the relationship between genomics and transcriptomics in AD and PD using clustering analysis of gene co-expression networks. They identified six clusters in AD and four in PD, which collaborate in each disease but exhibit low functional similarity, suggesting distinct biological processes in these diseases. Of the 15 commonly differentially expressed miRNAs reported between AD and PD, most appear to serve as a defence mechanism against neurotoxicity rather than playing a causal role in either AD or PD. The effects of glutamate toxicity support this hypothesis as a factor in AD [8].

1.2 Rationale

This thesis aims to explore the impact of nicotine on a subclass of long ncRNA, known as retrotransposons, specifically focusing on B2 SINE elements. Growing evidence suggests that these ncRNAs play a significant role in neural development, plasticity, cognitive diseases, and acute stress, such as neurotoxins [9]. Retrotransposons, belonging to class I transposable elements are distinguished from class II transposons based on their transposition mechanism. They mobilize throughout the genome via transcription into RNA intermediates, which are then reverse-transcribed and inserted at new genomic locations in a "copy-and-paste" manner [9]. Retrotransposons can be further categorized into two groups: those without long terminal repeats (LTRs), including long and short interspersed elements (LINEs and SINEs), and those with LTRs, known as endogenous retroviruses (ERVs).

Recent findings have shown that some short-interspersed element (SINE) RNAs can bind RNAP II and inhibit transcription, thereby regulating gene expression. This has been observed in murine B1 and B2 RNAs and human Alu RNA [15]. Murine cells contain at least four variants of B2 transcripts with different lengths: approximately 150, 180, 240, and 500 nt. In 2004, the secondary structure of the ~180 nt long transcripts was determined [16], consisting of three parts: (1) a long double-stranded region (1-72 nt) with an unwound section in the center, (2) a poorly structured region (73-153 nt) containing three small hairpins, and (3) a short 3'-terminal unstructured AU-rich region (154-178 nt) conserved in all SINEs.

RNAP III transcribes B2 RNA in the presence of TFIIIB and TFIIIC factors from their respective B2 SINE [17]. B2 functions by binding to genes and inhibiting translation elongation by Pol II [18]. Deletion analysis has demonstrated a 51 nt (81-131 nt) critical region for the functional binding of B2 onto Pol II. Transcriptional repression is most sensitive to the single-stranded region (99-115 nt) of B2 RNA complexed, requiring at least one hairpin structure for translation suppression [15]. B2 expression changes significantly during development, and its expression and processing respond to specific cellular stresses and diseases, such as viral infections, macular degeneration, cancer, and heat shock. A previous study [18] revealed that full-length B2 RNA undergoes specific endonucleolytic cleavage via interaction with the recruited EZH2 polycomb protein during heat shock responses. Cleaved B2 fragments exhibit dramatically reduced affinities for EZH2 (DKd 423 nM to >3,000 nM). They are released from target genes during the immediate early period of heat shock stress, allowing a higher percentage of elongating POL-II to reach the 3' termini of the target genes. The major cleavage site was identified at position 98, with minor cleavage sites at positions 77 and 33.

2. Objectives

Based on the above observations, we hypothesized that nicotine works as a neuroprotectant by means of altering the cleavage rate of B2. To this end:

- The first objective is to confirm that B2 is processed differently in APP transgenic mice, which are ideal models for AD.

- Following this, we wish to investigate the effects of chronic nicotine treatment in vivo on B2 transcript in the Mus musculus.
- Suppose there is evidence that B2 is differentially processed between nicotine and non-nicotine-treated mice. In that case, we wish to investigate how chronic nicotine affects gene expression of B2-suppressed genes previously linked to stress response [18].

3. Materials and Methods

3.1.1 APP Data

The APP transgenic Mus musculus hippocampus was isolated and sequenced by the Zovoilis lab at the University of Lethbridge to create an RNA library. Babita Gollen and Luke Saville were involved. Their protocol and results are pending publication. Yubo Cheng and Chris Isaac have previously analyzed the data.

3.1.2 Publicly Available Data Sources for ncRNA Bioinformatics Analysis

To identify relevant data for this study, we manually searched the published literature through Web of Science. We conducted NCBI keyword searches using terms such as "nicotine + brain + ncRNA" and "nicotine + neur* + ncRNA." We downloaded differentially expressed ncRNA data for nicotine-treated mice from the GEO database [10], using GEO accession numbers GSE117069 and GSE89899 as our data sources [19, 20].

The GSE117069 library, downloaded in February 2020, contains RNA samples aimed at studying the miRNA/mRNA-Seq of the habenula-interpeduncular withdrawal circuit [20]. We only used their control groups for our analysis. These control groups consisted of 6-week-old mice treated with nicotine tartrate (200 μg/ml nicotine base) or equivalent tartaric acid in their drinking water with saccharine (3 g/L) for 6 weeks. Fresh frozen brains were coronally sliced (~1 mm), and regions were dissected using a circular tissue punch (0.75-1mm diameter) in the Bregma ranges 1.8-0.8 mm for the NAc.

The GSE89899 library file, downloaded in January 2020, used GIN mice (FVB-Tg [GadGFP] 45704Swn) expressing enhanced green fluorescent protein (eGFP) [19]. Six male mice (20 g, 5-7 weeks) were divided into two groups for the GIN samples. Mice were implanted subcutaneously with an osmotic mini-pump that delivered 48 mg/kg/d nicotine hydrogen tartrate or saline vehicle for 14 days. Mice were decapitated, and brain slices (400 μm) were prepared using a vibratome. The cortexes were morphologically dissected and enzymatically digested by proNASE E in ACSF, then triturated. Cellular debris and molecular contaminants were removed from the resultant pieces. Fluorescent cells (Sst-positive) were carefully aspirated using a micropipette. Ten cells were aspirated each time, and 30 cells were collected from each mouse, totalling 90 cells from three mice in each group.

3.2 Tools Used for Analysis and Interpretation of Data

A full version of the commented pipeline used to download and process the genomic sequences for B2 RNA will be provided at the report's end and summarized in Figure 1. This section will focus on explaining the tools used and their purpose. The SRA Toolkit from NCBI is a collection of tools and libraries for using data in the International Nucleotide Sequence Database Collaboration (INSDC) Sequence Read Archives. Unless otherwise mentioned, data processing was performed on the Compute Canada DataBase (v.2.8.2-1) servers. Most of the fastq raw sequencing data was downloaded from the NCBI database using the SRA toolkit, while other data was manually downloaded from the NCBI website. The data used in this report came from previous research quantifying the expression of ncRNA in nicotine-treated mice [19, 20]. In the case of the interneuron data from GSE89899, the paired-end data fastq was manually downloaded as a single fastq file and then split.
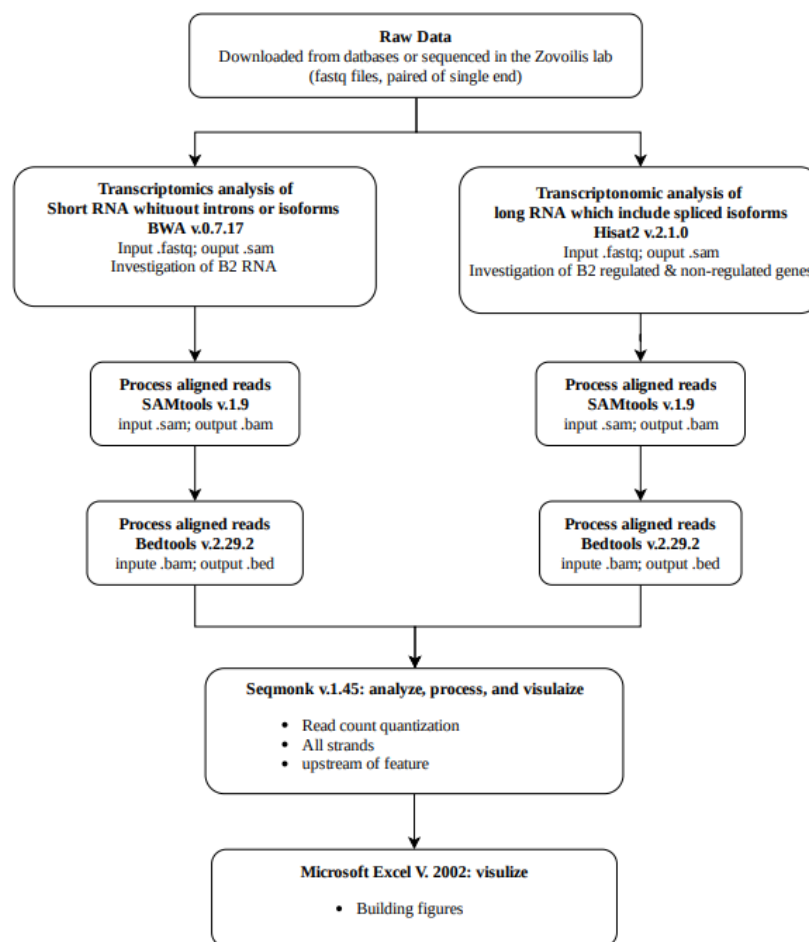

Figure 1. Flowchart describing the bioinformatics steps taken to analyze all the data in this report. In the first step of the flowchart, data is acquired by either downloading from NCBI or the Zovoilis lab. Following this, the data was either mapped with BWA for transcriptomic analysis of short RNA without introns, i.e. SINE B2 processing and levels, or the data was mapped using hisat2 for transcriptomic analysis of long RNA with splice isoforms to investigate of B2 and non-B2 regulated protein-coding RNA. The data was then aligned with Samtools and bedtools before being analyzed and processed with Seqmonk. Finally, the data was uploaded into Microsoft Excel for appropriate graphs and figures.

BWA is a software package for mapping low-divergent sequences against a large genome. Our research used BWA to map short RNAs from elements without introns against the mouse (mm10) reference genome. BWA's alignment search is bounded by a relatively low limit of mismatches in the alignment of the reads [21], making it ideal for detecting short nucleotide sequences to long reference sequences. Using BWA v.0.7.17 on the Compute Canada environment, the raw data from the fastq files were mapped against the mm10 mouse reference genome to produce sam files.

Like BWA, HISAT2 is also used for transcriptome analysis. However, HISAT2 is better suited for longer RNA analysis, including spliced isoforms of RNA. HISAT2 v.2.1.0 was used on the Compute Canada environment to align the fastq files against the mm10 mouse reference genome to produce sam files. Next, SAMtools v.1.9 was used to process the aligned reads of the sequenced data by converting the sam files into bam files and then using bedtools v.2.29.2 to convert the bam files into bed files.

Annotations were made to define the regions of investigation. The B2 annotation was made by downloading a query from the UCSC Table browser. The list of B2-regulated genes was isolated from the Zovoilis lab, specifically by Yubo Cheng. Seqmonk v.1.45 was used to visualize, process, and analyze the mapped sequence data in a local environment. The Mus musculus GRCm38 (2012-08-06) mouse genome assembly was imported from the seqmonk server to analyze the sequences. All bed files from both cohorts were uploaded.

A quantitative analysis was performed using Read count quantitation, which counts the number of reads that overlap with all strands. An average probe region can be visualized using the probe trend plot option. In both cohorts, data were grouped in replicate sets, representing biological replicates of related samples. Replicate Sets are ideally used to provide sample grouping for statistical filters that compare two groups of samples.

4. Results

4.1 Increased processing of B2 in 6-month-old APP mice

Fig. 2 reflects the cumulative quantitation of the read counts that overlap with known immediate B2-regulated genes of the Mus musculus genome using long reads isolated from the hippocampus in 6-month-old APP transgenic mice. Compared with their control counterparts, an increase of ~9 (± 1) % in B2 levels is seen in vivo for the 6-month-old APP transgenic mice. The Kolmogorov-Smirnov (KS) comparison of the two data sets reveals a significant difference between the cumulative distributions (D = 0.6770, P < 0.05), suggesting that dementia produces different B2 RNA transcriptome signatures in the hippocampus. The total number of reads in the APP experiment library after mapping against the Mus musculus genome using BWA and SAMtools is indicated in Table 1.
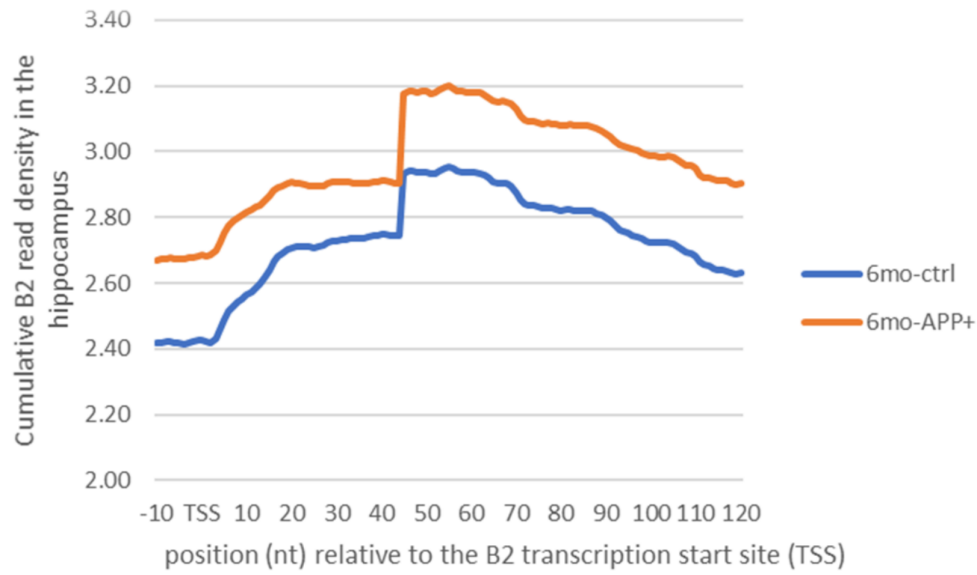
Figure 2. Different B2 RNA transcriptome signatures in the hippocampus of APP Mus musculus brains. Distribution of paired-end RNAseq reads from samples prepared to form a long reads library within the functionally critical binding region of B2 across the metagene profile of all B2 elements aligned to their TSS, which was taken on an average between all the known loci for B2 elements in the Mus musculus genome. The absolute distance from the transcription start site (TSS) is shown on the x-axis. The y-axis is a normalized cumulative sum of the reads in the sequenced data that overlap.

Table 1. Read count after aligning the APP library for hippocampal cells against the Mus musculus genome using BWA and SAMtools.

File name	Info	Reads
14-15LR	6mo-APP	56670769
18-19LR	6mo-APP	54430927
22-23LR	6mo-APP	54851131
58-59LR	6mo-ctrl	52551224
62-63LR	6mo-ctrl	41728390
66-67LR	6mo-ctrl	57120910

4.2 Increased processing of B2 in nicotine-treated mice

Fig. 3 shows the relative quantitation of read counts overlapping with known B2 regions of the Mus musculus genome using long reads from the GSE89899 library, which isolated hippocampal cells. The mean of the distribution is at 98 ($\pm$ 52) nt, consistent with previous research indicating that B2 is cleaved at position 98 by EZH2 [18]. An increase in B2 levels is seen in vivo for nicotine-treated samples versus their control counterparts. The KS comparison of the two data sets reveals a significant difference between the relative read count distributions (D = 0.2275, P < 0.05), confirming that nicotine significantly affects B2 RNA levels in interneurons of the brain. The total number of reads in the GSE89899 library after mapping against the Mus musculus genome using BWA and SAMtools is indicated in Table 2.
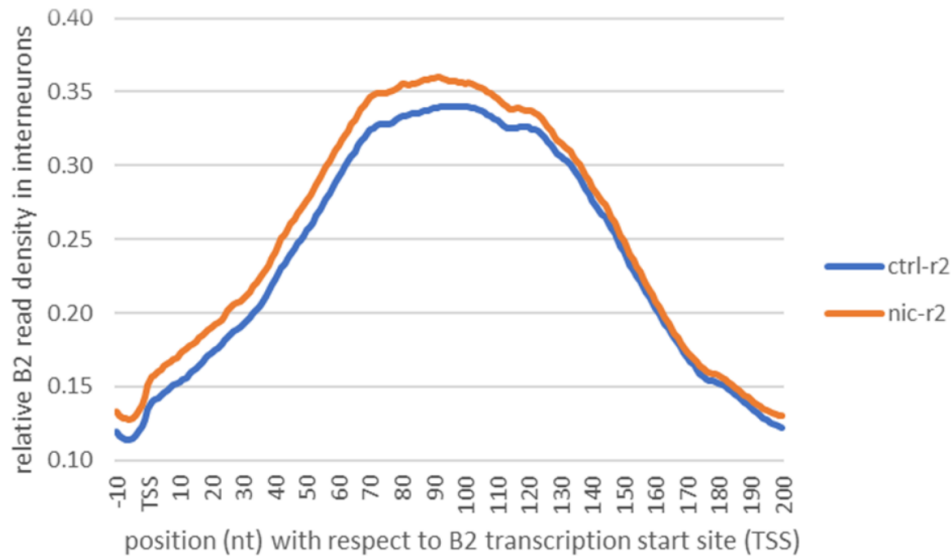
Figure 3. Increased in B2 levels and processing in interneurons of nicotine-treated mice. Distribution of the R2 paired-end RNA-seq reads from samples of interneurons of Mus musculus brains, prepared from a long reads library, within the functionally critical binding region of B2 across the metagene profile of all B2 elements aligned to their TSS, which was taken on an average between all the known loci for B2 elements in the Mus musculus genome. The absolute distance from the transcription start site (TSS) is shown on the x-axis. The y-axis is a corrected, normalized average of reads in the sequenced data that overlap.

Table 2. Read count after aligning the GSE89899 library containing interneurons of nicotine-treated mice against the Mus musculus genome using BWA and SAMtools.

File name	SRA code	Reads
sst-1	SRR5026253	30550384
sst-2	SRR5026254	26171129
sst-3	SRR5026255	26603675
sst-nic-1	SRR5026256	24783977
sst-nic-2	SRR5026257	24314301
sst-nic-3	SRR5026258	35790377

Fig. 4 shows the relative quantitation of read counts overlapping with known B2 regions of the Mus musculus genome using short reads isolated from the Nucleus Accumbens (NAc) in the GSE117069 library. Compared with their control counterparts, an increase of 85.6 (± 41.3) % in B2 level/processing is seen in vivo for the nicotine-treated replicate set. The KS comparison of the two data sets reveals a significant difference between the distributions (D = 0.7702, P < 0.05), confirming that nicotine significantly affects B2 RNA processing in the NAc. The total number of reads in the GSE117069 library after mapping against the Mus musculus genome using BWA and SAMtools is indicated in Table 3.
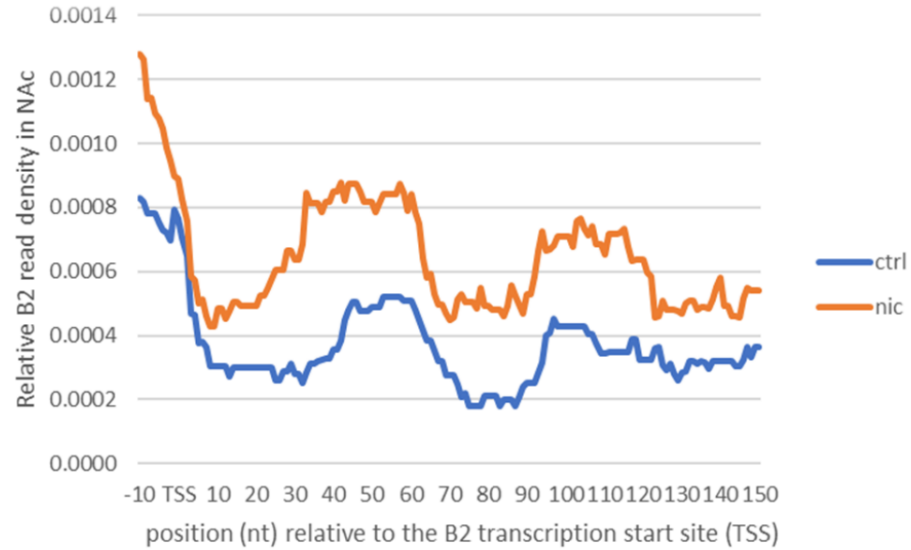
Figure 4. Increased in B2 levels and processing in the NAc of nicotine-treated mice. Distribution of the single-end RNA-seq reads from samples within the NAc of Mus musculus brains, filtered for small RNA, within the functionally critical binding region of B2 across the metagene profile of all B2 elements aligned to their TSS. The distribution was taken on an average between all the known loci for B2 elements in the Mus musculus genome. The absolute distance relative to the B2 transcription start site (TSS) is shown on the x-axis. The y-axis is a corrected, normalized average of reads in the sequenced data that overlap. Sharp discontinuities indicate either artifact or position where B2 is processed.

Table 3. Read count after aligning the GSE117069 library containing NAc neurons of nicotine-treated mice against the Mus musculus genome using BWA and SAMtools.

File name	SRA code	Reads
NAc_miRNA_TA5	SRR7518501	23853269
NAc_miRNA_TA4	SRR7518500	16001905
NAc_miRNA_TA3	SRR7518499	22876769
NAc_miRNA_TA2	SRR7518498	16296608
NAc_miRNA_TA1	SRR7518497	17573193
NAc_miRNA_Nic5	SRR7518496	19638403
NAc_miRNA_Nic3	SRR7518495	23939235
NAc_miRNA_Nic3	SRR7518494	30287696
NAc_miRNA_Nic2	SRR7518493	18403776

Fig. 5 shows the cumulative quantitation of read counts overlapping with known immediate B2-regulated genes of the Mus musculus genome using long reads from the GSE89899 library, which isolated interneuron cells. The data reveals an average expression increase of 9.5 ($\pm$ 2.7) % for nicotine-treated samples. The KS comparison on the first 1000 bp downstream of the TSS reveals a significant difference between the two data sets (D = 0.4396, P < 0.05). Fig. 6 shows the cumulative quantitation of read counts overlapping with all other genes of the Mus musculus genome, taken across the first 2000 nt from the TSS, using the same data as the previous figure. The control genes unaffected by immediate B2 regulation were more highly expressed by an additional 3.8 ($\pm$ 1.4) % over the nicotine replicate set counterpart. The KS comparison on the first 1000 bp downstream of the TSS reveals a significant difference between

the two data sets (D = 0.3247, P < 0.05). These graphs indicate that nicotine significantly affects the expression of immediate-B2 regulated genes and a concomitant significant relationship on non-B2 regulated genes. The total number of reads in the GSE89899 library after mapping against the Mus musculus genome using Hisat2 and SAMtools is indicated in Table 4.
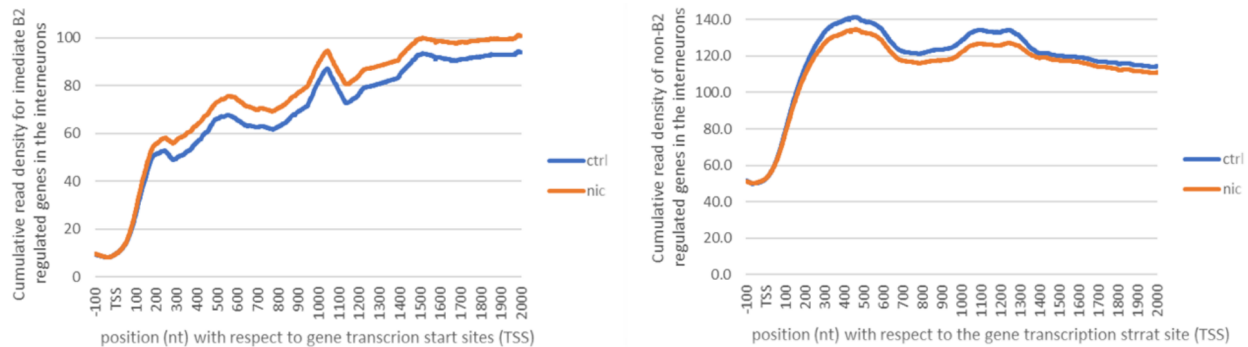

Figure 5&6. Differently expressed genes associated with B2 (left) or its control (right) in the interneurons of mice. Distribution of paired-end RNA-seq reads for the expressed genomic data from the interneurons of Mus musculus brains, prepared from long reads library. The absolute distance to the gene transcription start site (TSS) is shown on the x-axis. The y-axis is a normalized cumulative sum of the reads in the sequenced data that overlap. Fig. 5 (left) Distribution is taken as the cumulative expression of reads over the known loci of immediate B2 regulated genes; fig. 6 (right) or else taken as the cumulative expression of reads over the known loci of all known non-immediate B2 regulated genes

Table 4. Read count after aligning the GSE89899 library containing interneurons of nicotine-treated mice against the Mus musculus genome using Hisat2 and SAMtools.

File name	SRA code	Reads
sst-1	SRR5026253	62247120
sst-2	SRR5026254	53342568
sst-3	SRR5026255	54084328
sst-nic-1	SRR5026256	50176394
sst-nic-2	SRR5026257	48919801
sst-nic-3	SRR5026258	72860543

Discussion & Conclusion

The ability to mount a rapid and effective response to neurotoxins is crucial for survival, and failure to do so can lead to various diseases, including dementia. Previous research has investigated the similarities between Alzheimer's disease (AD) and Parkinson's disease (PD). Although these diseases appear to involve different biological processes, 15 common miRNAs found in both conditions have been suggested to serve as a defence mechanism against brain toxicity. In this study, we examined the effects of nicotine on B2 elements, which have been shown to change expression levels in response to acute and chronic stressors such as dementia or exposure to toxins.

We found that B2 processing increased in APP transgenic mice, a model for AD, as well as in interneurons and the NAc during chronic nicotine treatment. The increased processing allowed for enhanced translation and expression of immediate B2-regulated genes compared to non-B2-regulated genes. Our findings suggest that one of the mechanisms by which nicotine

functions as a neuroprotectant against dementia is by chronically increasing the expression of stress response genes, which serve as a defence mechanism against neurotoxicity, such as chronic excitotoxicity that would typically lead to dementia.

However, our study has several limitations that need to be acknowledged. The presence of artifacts in the sequencing data, such as the discontinuity at 125 nt and 170 nt, could have affected the interpretation of our results. These artifacts might have arisen due to biases in PCR amplification, biases in the ability of the sequencer to sequence each variant, or stochasticity in the abundance of molecules in the sample [22]. Our study also relied on publicly available data, which might not have been ideal for our research question. Many studies have investigated the harmful effects of nicotine on the body, brain development, addiction, and withdrawal, but few have focused on its potential neuroprotective effects against dementia. This limited the availability of suitable tissue samples for our investigation.

Yet another limitation was the preparation method of the RNA-seq libraries, which influenced the results obtained. Different library preparation methods emphasize different aspects of the expression profiles of B2 and genes, which might have affected our ability to isolate changes in the levels and processing of SINE B2 RNA [23-27]. Despite analyzing the data from the interneuron cell library, we could not identify a clear discontinuity in the levels or processing of SINE B2 RNA, which would have indicated the location of B2 processing.

In conclusion, our findings demonstrate that B2 processing increases in APP mice, a model for AD, and in interneurons and the NAc during chronic nicotine treatment. This increased processing allows for the enhanced translation and expression of immediate B2-regulated genes compared to non-B2-regulated genes. Our results suggest that one mechanism by which nicotine functions as a neuroprotectant against dementia is by chronically increasing the expression of stress response genes that act as a defence mechanism against neurotoxicity. These findings provide further evidence supporting the potential use of nicotine as both a treatment and a preventive measure against dementia. Future work could investigate the impact of other recreational drugs, such as alcohol and marijuana, on SINE elements, including ALU, in humans. Such research could contribute to developing treatments and proactive measures against neurodegenerative diseases.

Citations
1. Yang, J., et al., Age- and Nicotine-Associated Gene Expression Changes in the Hippocampus of APP/PS1 Mice. Journal of Molecular Neuroscience, 2019. 69(4): p. 608-622.
2. Rana, P., et al., Evaluation of the Common Molecular Basis in Alzheimer's and Parkinson's Diseases. International Journal of Molecular Sciences, 2019. 20(15): p. 27.
3. Vasili, E., A. Dominguez-Meijide, and T.F. Outeiro, Spreading of alpha-Synuclein and Tau: A Systematic Comparison of the Mechanisms Involved. Frontiers in Molecular Neuroscience, 2019. 12: p. 23.
4. Quik, M., X.A. Perez, and T. Bordia, Nicotine as a potential neuroprotective agent for Parkinson's disease. Movement Disorders, 2012. 27(8): p. 947-957.
5. Xie, A.M., et al., Shared Mechanisms of Neurodegeneration in Alzheimer's Disease and Parkinson's Disease. Biomed Research International, 2014: p. 8.
6. Fratiglioni, L. and H.X. Wang, Smoking and Parkinson's and Alzheimer's disease: review of the epidemiological studies. Behavioural Brain Research, 2000. 113(1-2): p. 117-120.

7. Picciotto, M.R. and M. Zoli, Nicotinic receptors in aging and dementia. Journal of Neurobiology, 2002. 53(4): p. 641-655.
8. Lewerenz, J. and P. Maher, Chronic Glutamate Toxicity in Neurodegenerative DiseasesWhat is the Evidence? Frontiers in Neuroscience, 2015. 9: p. 20.
9. Dunker, W., et al., Recognizing the SINEs of Infection: Regulation of Retrotransposon Expression and Modulation of Host Cell Processes. Viruses-Basel, 2017. 9(12): p. 9.
10. Mattick, J.S., The central role of RNA in human development and cognition. Febs Letters, 2011. 585(11): p. 1600-1616.
11. Tan, L., J.T. Yu, and N. Hu, Non-coding RNAs in Alzheimer's disease. Mol Neurobiol, 2013. 47(1): p. 382-93.
12. Lukiw, W.J., Micro-RNA speciation in fetal, adult and Alzheimer's disease hippocampus. Neuroreport, 2007. 18(3): p. 297-300.
13. Wang, W.X., et al., The expression of microRNA miR-107 decreases early in Alzheimer's disease and may accelerate disease progression through regulation of beta-site amyloid precursor protein-cleaving enzyme 1. Journal of Neuroscience, 2008. 28(5): p. 1213-1223.
14. Mus, E., P.R. Hof, and H. Tiedge, Dendritic BC200 RNA in aging and in Alzheimer's disease. Proceedings of the National Academy of Sciences of the United States of America, 2007. 104(25): p. 10679-10684.
15. Burenina, O.Y., T.S. Oretskaya, and E.A. Kubareva, Non-coding RNAs As Transcriptional Regulators In Eukaryotes. Acta Naturae, 2017. 9(4): p. 13-25.
16. Espinoza, C.A., J.A. Goodrich, and J.F. Kugel, Characterization of the structure, function, and mechanism of B2 RNA, an ncRNA repressor of RNA polymerase II transcription. Rna-a Publication of the Rna Society, 2007. 13(4): p. 583-596.
17. Espinoza, C.A., et al., B2 RNA binds directly to RNA polymerase II to repress transcript synthesis. Nature Structural & Molecular Biology, 2004. 11(9): p. 822-829.
18. Zovoilis, A., et al., Destabilization of B2 RNA by EZH2 Activates the Stress Response. Cell, 2016. 167(7): p. 1788-+.
19. Yang, J., et al., Chronic nicotine differentially affects murine transcriptome profiling in isolated cortical interneurons and pyramidal neurons. Bmc Genomics, 2017. 18: p. 11.
20. Casserly, A.P., et al., Integrated miRNA-/mRNA-Seq of the Habenulo-Interpeduncular Circuit During Acute Nicotine Withdrawal. Scientific Reports, 2020. 10(1): p. 14.
21. Keel, B.N. and W.M. Snelling, Comparison of Burrows-Wheeler Transform-Based Mapping Algorithms Used in High-Throughput Whole-Genome Sequencing: Application to Illumina Data for Livestock Genomes. Frontiers in Genetics, 2018. 9: p. 6.
22. Nugmanov, G.A., et al., A Pipeline for the Error-Free Identification of Somatic AluInsertions in High-Throughput Sequencing Data. Molecular Biology, 2019. 53(1): p. 138-146.
23. Goldberg, L.R., et al., Paternal nicotine enhances fear memory, reduces nicotine administration, and alters hippocampal genetic and neural function in offspring. AddictionBiology: p. 14.
24. Silva, C.P., et al., The influence of adolescent nicotine exposure on ethanol intake andbrain gene expression. Plos One, 2018. 13(6): p. 30.
25. Jung, Y., et al., An epigenetic mechanism mediates developmental nicotine effects on neuronal structure and behavior. Nature Neuroscience, 2016. 19(7): p. 905-914.
26. Wang, G.Q., et al., Persistence of Smoking-Induced Dysregulation of MiRNA Expressionin the Small Airway Epithelium Despite Smoking Cessation. Plos One, 2015. 10(4): p.18.
27. Lauterstein, D.E., et al., Frontal Cortex Transcriptome Analysis of Mice Exposed toElectronic Cigarettes During Early Life Stages. International Journal of Environmental Research and Public Health, 2016. 13(4): p. 14.